Discontinuous Finite-Element Approximations for the Analysis of Shock Waves in Nonlinearly Elastic Materials

L. C. WELLFORD, JR.

Department of Civil Engineering, University of Southern California, Los Angeles, California 90007

AND

J. T. ODEN

Texas Institute for Computational Mechanics, The University of Texas, Austin, Texas 78712

Received January 17, 1975

In this paper a new technique for calculating shock waves in nonlinear materials using finite element methods is described. The basic feature of the technique is the use of finite elements with built-in discontinuities. This requires the introduction of additional parameters which are taken to be the strength of the shock and the location of the shock front in an element. A variational principle for shock wave propagation with jump conditions is derived, and this is used together with discontinuous trial functions to produce equations of motion and equations for the growth and decay of shocks. The method is applied to a number of representative nonlinear problems, and numerical results and comparisons are indicated. Computationally the technique appears to offer a number of advantages over shock smearing schemes including a quite accurate description of the structure of the shock front.

1. INTRODUCTION

There is an important shortcoming of conventional finite-element Galerkin schemes when applied to general nonlinear elastodynamics problems. Unless special precautions are taken, these schemes depict discontinuous solutions as being quite smooth. In addition, temporal operators used to stabilize these conventional schemes often are accompanied by unacceptable degrees of artificial viscosity. This is particularly serious in shock wave problems wherein a sharp definition of the shock front, its strength, and rate-of-decay are required. On the other hand, global theories of nonlinear hyperbolic equations must be developed in a distributional setting, and it is from such weak or variational forms of

179

boundary- and initial-value problems that the entire theory of Galerkin approximations emerges. It would seem, therefore, that the most effective—if not the most natural—way to approximate nonlinear wave phenomena would be to develop schemes which employ the pholosphy and attactive features of Galerkin methods but which are also capable of modeling sharp discontinuities at various wave fronts. It is on this observation that the present investigation is based.

In this paper we develop a numerical scheme and associated computational procedures for the approximation of shock waves in one-dimensional nonlinearly elastic bodies using discontinuous finite elements, and we describe a number of specific applications of these ideas to representative problems. The basic idea is to decompose the domain of the nonlinear initial-value problem into collections of shockless domains meeting at surfaces of discontinuity where certain jump conditions must be applied. Conventional finite-element methods are used to model the behavior in the shockless domains, whereas special finite elements are used to model the behavior in a boundary layer of elements surrounding the shock front. In a companion paper [1] we have developed a fairly complete mathematical theory for such approximations, without applications and without examples of specific families of discontinuous shape functions. The present paper is aimed at further resolving this theory and at the development and application of specific types of approximations.

Following this introduction, we review certain fundamental relationships in the theory of shock waves. In Section 3, we develop special variational forms of the equations of motion for the nonlinear elastic solid in the presence of a shock. These form the basis for all of our special Galerkin schemes. In Section 4, we develop a space of discontinuous finite-element models and, using the variational principle of Section 3, construct an associated semidiscrete finite-element/Galerkin model for the propagation of shock waves. In Section 5, several approximations for the acceleration fields of material particles are introduced using finite differences in time. In Sections 6 and 7 fully discrete approximations for shock propagation are obtained by implementing the finite-element/Galerkin scheme of Section 4 with the approximations for the temporal operator of Section 5. In Section 8 we discuss the global formulation of the problem and present various special procedures to be used to handle the reflection of nonlinear waves, etc. In Section 9, several numerical examples concerned with the growth and reflection of shock waves are presented.

2. SOME PRELIMINARIES

In this section we consider some basic relationships which are standard tools in the theoretical aspects of the problem of shock propagation.

We begin by considering one-dimensional motions of a continuous body B.

In particular, let $I \subset B$ denote a set of material particles X in motion relative to a fixed coordinate frame x. At any time t, the motion of a particle $X \in I$ relative to its position at $t = 0$ is given by a function χ,

$$x = \chi(X, t), \qquad (2.1)$$

and, for simplicity, we choose $\chi(X, 0) = X$, The displacement of particle X at time t is then

$$u(X, t) = x - X = \chi(X, t) - X \qquad (2.2)$$

and the velocity and gradient of displacement at X at time t are denoted

$$\dot{u}(X, t) = \partial u(X, t)/\partial t, \qquad u_X(X, t) = \partial u(X, t)/\partial X. \qquad (2.3)$$

Here the partial derivatives are to be interpreted in a generalized sense, i.e., in the sense of distributions. We are interested in describing the motion of B over some finite time interval $0 \leqslant t \leqslant T$, although T may be very large.

From the onset, we must anticipate the possibility that various fields may suffer discontinuities of one type or another during the time period $[0, T]$. To describe such surfaces (points) of discontinuity, let

$$Q = \{Y_k\}_{k=0}^{N} \qquad (2.4)$$

denote a set of $N + 1$ real-valued functions from $[0, T]$ into $\mathbb{R}$ ($\mathbb{R}$ is the real line) such that for each $t \in [0, T]$, Q is a partition of I; i.e., if $0 = \inf\{I\}$, $a = \sup\{I\} < \infty$, then $0 \leqslant Y_0 < Y_1 < \cdots < Y_N \leqslant a$, $a \in \mathbb{R}$.
The quotient set

$$I/Q = \bigcup_{i=1}^{N} J_i(t), \qquad t \in [0, T], \qquad (2.5)$$

describes the decomposition of I into a number of open *shockless domains*

$$J_i(t) = (Y_{i-1}(t), Y_i(t)), \qquad 1 \leqslant i \leqslant N, \qquad (2.6)$$

and a number of singular surfaces $Y_i(t)$ on which jump discontinuities may arise.
The *intrinsic speed* of the ith wave is then

$$V_i = dY_i(t)/dt, \qquad 1 \leqslant i \leqslant N - 1, \qquad (2.7)$$

and the *jump* of any quantity ψ at the surface (point) Y_i is denoted

$$[\![\psi]\!]_{Y_i} \equiv \psi(Y_i^+, t) - \psi(Y_i^-, t). \qquad (2.8)$$

We also define the *average* of ψ at the surface Y_i as

$$\bar{\psi}_i \equiv \tfrac{1}{2}[\psi(Y_i{}^+, t) + \psi(Y_i{}^-, t)]. \tag{2.9}$$

Thus

$$\psi(Y_i{}^+, t) = \bar{\psi}_i + \tfrac{1}{2}[\![\psi]\!]_{Y_i},$$
$$\psi(Y_i{}^-, t) = \bar{\psi}_i - \tfrac{1}{2}[\![\psi]\!]_{Y_i}. \tag{2.10}$$

We next introduce the following notation.

$\sigma(X, t) =$ the first Piola–Kirchhoff stress,

$\rho(X) =$ the density of B in the reference configuration,

$e(X, t) =$ the specific internal energy,

$\xi(X, t) =$ the specific entropy,

$q(X, t) =$ the heat flux,

$\theta(X, t) =$ the absolute temperature,

$f(X, t) =$ the body force density.

All of these denote values at particle X at time t, $X \in I \subset B$, $t \in [0, T]$. Then we formulate the shock propagation problem in its free boundary form as follows. Find the set $\{u, \sigma, e, q, \xi, \theta\}$ such that

$$\left.\begin{array}{r}\rho \ddot{u} - \sigma_X - f = 0,\\ \dot{e} - \sigma \dot{u}_X - q_X = 0,\\ \theta \dot{\xi} - q_X + (q\theta_X/\theta) \geqslant 0,\end{array}\right\} \text{ on } J_i, \qquad i = 1, \dots, N,$$

and

$$\left.\begin{array}{r}\rho V_i[\![\dot{u}]\!]_{Y_i} + [\![\sigma]\!]_{Y_i} = 0,\\ \tfrac{1}{2}\rho V_i[\![\dot{u}^2]\!]_{Y_i} + V_i[\![e]\!]_{Y_i} + [\![\sigma \dot{u}]\!]_{Y_i} + [\![q]\!]_{Y_i} = 0,\\ V_i[\![\xi]\!]_{Y_i} - [\![q/\theta]\!]_{Y_i} \geqslant 0,\end{array}\right\} \text{ on } Y_i, \qquad i = 1, \dots, N-1. \tag{2.11}$$

In addition to $(2.11)_4$, $(2.11)_5$, and $(2.11)_6$, which are the momentum, energy, and entropy jump conditions at the free boundary or shock, a kinematic compatibility equation can be shown to hold at the shock. For the one-dimensional domain the kinematical compatibility condition [2] takes the form at Y_i:

$$[\![\dot{u}]\!]_{Y_i} = -V_i[\![u_X]\!]_{Y_i}. \tag{2.12}$$

From the momentum jump condition $(2.11)_4$ and the kinematical compatibility condition (2.12) we can develop a well-known formula specifying the intrinsic velocity of a shock wave [3]:

$$V_i{}^2 = [\![\sigma]\!]_{Y_i}/\rho[\![u_X]\!]_{Y_i}, \qquad i = 1, \dots, N-1. \tag{2.13}$$

3. VARIATIONAL EQUATIONS FOR SHOCK WAVES

In this section we shall record for future reference the basic balance laws of mechanics in a weak or variational form, and show how these can be used to develop a weak conservation form of the equations of motion (i.e., a weak form of the principle of balance of linear momentum) complete with the appropriate jump conditions.

We may write the following balance laws governing thermomechanical behavior of B.

(i) Balance of linear momentum:

$$\sum_{i=1}^{N} \int_{J_i} \left\{ \frac{\partial}{\partial t} (\rho \dot{u}) - f \right\} dX + \sum_{i=1}^{N-1} \rho V_i [\![\dot{u}]\!]_{Y_i} = \{ \sigma(\cdot, t) \} |_{X=0}^{X=a}. \tag{3.1}$$

(ii) Conservation of energy:

$$\frac{1}{2} \sum_{i=1}^{N} \int_{J_i} \left[\frac{\partial}{\partial t} (\rho \dot{u}^2 + 2e) - 2\rho f \dot{u} \right] dX + \frac{1}{2} \sum_{i=1}^{N-1} \rho V_i [\![\dot{u}^2]\!]_{Y_i} + \sum_{i=1}^{N-1} V_i [\![e]\!]_{Y_i}$$

$$= \{ \sigma(\cdot, t) \dot{u}(\cdot, t) + q(\cdot, t) \} |_{X=0}^{X=a}. \tag{3.2}$$

(iii) The Clausius–Duhem inequality:

$$\sum_{i=1}^{N} \int_{J_i} \frac{\partial \xi}{\partial t} dX + \sum_{i=1}^{N-1} V_i [\![\xi]\!]_{Y_i} - \left\{ \frac{q(\cdot, t)}{\theta(\cdot, t)} \right\} \Big|_{X=0}^{X=a} \geqslant 0. \tag{3.3}$$

In these laws we use the notation

$$\{ \psi(\cdot, t) \} |_{X=0}^{X=a} = \psi(a, t) - \psi(0, t). \tag{3.4}$$

LEMMA 3.1. *The identities*

$$\{ \psi(\cdot, t) \} |_{X=0}^{X=a} = \sum_{i=1}^{N} \int_{J_i} \frac{\partial \psi}{\partial X} dX - \sum_{i=1}^{N-1} [\![\psi]\!]_{Y_i} \tag{3.5}$$

hold for any function ψ whose derivative ψ_X is integrable on $\bigcup_{i=1}^{N} J_i$; moreover,

$$[\![\sigma \dot{u}]\!]_{Y_i} = \bar{\sigma}_i [\![\dot{u}]\!]_{Y_i} + \bar{\dot{u}}_i [\![\sigma]\!]_{Y_i} \tag{3.6}$$

and

$$[\![\dot{u}^2]\!]_{Y_i} = 2\bar{\dot{u}}_i [\![\dot{u}]\!]_{Y_i}. \tag{3.7}$$

Proof. These equalities follow immediately from the definitions. ∎

When field variables in (3.1) and (3.2) are sufficiently smooth in the shockless subdomains, the following local energy laws hold.

$$\dot{e}(X, t) - \sigma(X, t)\,\dot{u}_X(X, t) - q_X(X, t) = 0, \qquad \forall X \in \bigcup_{i=1}^{N} J_i, \quad \forall t \in [0, \infty); \quad (3.8)$$

$$V_i[\![e]\!]_{Y_i} + \bar{\sigma}_i[\![\dot{u}]\!]_{Y_i} + [\![q]\!]_{Y_i} = 0, \qquad \forall Y_i \in Q. \tag{3.9}$$

We need not assume that such strong conditions hold. We shall say that energy is conserved in a *locally integrable sense* whenever

$$\int_{J_i} (\dot{e} - \sigma\dot{u}_X - q_X)\,dX = 0, \qquad \forall J_i \subset I; \tag{3.10}$$

$$V_i[\![e]\!]_{Y_i} + \bar{\sigma}_i[\![\dot{u}]\!]_{Y_i} + [\![q]\!]_{Y_i} = 0, \qquad \forall Y_i \in Q. \tag{3.11}$$

In (3.10), the derivatives u_X and q_X are to be interpreted in the sense of distributions.

THEOREM 3.1. *Let energy be conserved in the locally integrable sense of* (3.10) *and* (3.11). *Then linear momentum is balanced in a weak sense if and only if*

$$\sum_{i=1}^{N} \int_{J_i} (\rho\ddot{u} - \sigma_X - \rho f)v\,dX + \sum_{i=1}^{N-1} \{\rho V_i[\![\dot{u}]\!]_{Y_i} + [\![\sigma]\!]_{Y_i}\}\,\bar{v}_i = 0 \tag{3.12}$$

for every velocity field v satisfying the kinematical constraints on the motion of the body B.

Proof. The principle of conservation of energy (3.2) can, with the aid of Lemma 3.1, be rewritten in the form

$$\sum_{i=1}^{N} \int_{J_i} (\rho\ddot{u}\dot{u} + \dot{e} - \rho f\dot{u})\,dX + \sum_{i=1}^{N-1} (\rho V_i[\![\dot{u}]\!]_{Y_i}\,\bar{\dot{u}}_i + V_i[\![e]\!]_{Y_i})$$

$$= \sum_{i=1}^{N} \int_{J_i} \left(\frac{\partial}{\partial X}(\sigma\dot{u}) + q_X\right)dX - \sum_{i=1}^{N} (\bar{\sigma}_i[\![\dot{u}]\!]_{Y_i} + \bar{\dot{u}}_i[\![\sigma]\!]_{Y_i} + [\![q]\!]_{Y_i}).$$

Introducing (3.10) and (3.11), we have

$$\sum_{i=1}^{N} \int_{J_i} (\rho\ddot{u} - \sigma_X - \rho f)\dot{u}\,dX + \sum_{i=1}^{N-1} (\rho V_i[\![\dot{u}]\!]_{Y_i}\,\bar{\dot{u}}_i + [\![\sigma]\!]_{Y_i}\,\bar{\dot{u}}_i) = 0.$$

Recognizing that $\dot{u}$ can be varied independently of $\ddot{u}$ and the other variables, we replace it by an arbitrary kinematically admissible velocity field v to obtain (3.12). ∎

We shall call (3.12) a *weak conservation form* of the balance of linear momentum

including jump terms associated with the shock problem. An alternate version of this weak conservation form is presented in the following corollary.

COROLLARY 3.1. *Let the conditions of Theorem 3.1 hold. Then, for every kinematically admissible velocity field v,*

$$\sum_{i=1}^{N} \int_{J_i} [(\rho\ddot{u} - \rho f)v + \sigma v_X] \, dX + \sum_{i=1}^{N-1} (\rho V_i [\![\dot{u}]\!]_{Y_i} \bar{v}_i - \bar{\sigma}_i [\![v]\!]_{Y_i}) = \{\sigma(\cdot, t) \, v(\cdot)\}|_{X=0}^{X=a} .$$
$$(3.13)$$

Proof. This alternate form is obtained from (3.12) by integrating the term $\sigma_X v$ by parts and using (3.5) and (3.6) of Lemma 3.1. ∎

We have developed the *weak conservation forms* (3.12) and (3.13) strictly from physical arguments. However, we prefer to introduce an alternate but equivalent formulation here. Let $H^1(I)$ be the space of functions which have $u \in L_2(I)$ and $u_X \in L_2(I)$, where $L_2(I)$ is the space of square integrable functions. $H^1(I)$ is provided with the norm

$$\| u \|_{H^1(I)}^2 = \int_I (| u |^2 + | u_X |^2) \, dX.$$

We denote by $H_0^1(I)$ the space of functions in $H^1(I)$ which satisfy homogeneous boundary conditions. That is, $H_0^1(I) = \{v : v \in H^1(I), v(0) = v(a) = 0\}$. In addition we let $\mathscr{H} = \{v : v \in \prod_{i=1}^{N} H^1(J_i), v \in L_2(I)\}$ and $\mathscr{\mathring{H}} = \{v : v \in \mathscr{H}, v(0) = v(a) = 0\}$. Then a *variational formulation for shock propagation* is defined as follows. Find $u \in H_0^1(I)$ such that

$$\sum_{i=1}^{N} \int_{J_i} [(\rho\ddot{u} - \rho f)v + \sigma v_X] \, dX + \sum_{i=1}^{N-1} (\rho V_i [\![u]\!]_{Y_i} \bar{v}_i - \bar{\sigma}_i [\![v]\!]_{Y_i})$$

$$= \{\sigma(\cdot, t) \, v(\cdot)\}|_{x=0}^{x=a}, \qquad \forall v \in \mathscr{\mathring{H}}. \qquad (3.14)$$

It can be shown that if $f \in L_2(J_i)$, $i = 1,..., N - 1$, then the formulation (3.14) is equivalent to solving (2.11), the problem in its free boundary form. That is, (3.14) is the variational formulation of the free boundary problem of shock propagation.

4. DISCONTINUOUS FINITE-ELEMENT MODELS

Conventionally, finite-element approximations of a function $u(X, t)$ are constructed by partitioning the domain I into a finite number E of connected subdomains over which the function is interpolated via simple polynomials. By

connecting the subdomains I_e togetheer and matching values of the local inter-
polants and possibly certain derivatives, at the points of intersection of the elements
(i.e., the nodal points), a system of *global* "shape" or interpolation functions
$\{\phi_\alpha(X)\}_{\alpha=1}^{L+1}$ are generated which, for each $t \in [0, T]$, form the basis of a finite-
dimensional space of functions. In such a construction, the approximation of the
displacement field u is of the form

$$U(X, t) = \sum_{\alpha=1}^{G} A^\alpha(t)\, \phi_\alpha(X) \tag{4.1}$$

and the velocity is

$$\dot{U}(X, t) = \sum_{\alpha=1}^{G} \dot{A}^\alpha(t)\, \phi_\alpha(X). \tag{4.2}$$

The construction of approximate schemes for shock problems using represen-
tations such as (4.1) and (4.2) leads to an immediate paradox: $U(X, t)$ can be made
continuous in X by an appropriate choice of the global basis functions $\phi_\alpha(X)$, but
these same functions depict the behavior of the velocity $\dot{U}(X, t)$, which is known
to have discontinuities at the shock front. Thus, without some deliberate modi-
fications of the conventional finite-element/Galerkin method, we will obtain
schemes of the "shock-smearing" type, which depict a continuous but rapidly
changing variation of velocity and displacement gradient over a shock front.

Instead of following this conventional approach, we shall construct a Galerkin
scheme which contains an explicit definition of the wave front. We begin by letting
P denote a partition of the particles I defined by the G nodal points

$$0 = X^0 < X^1 < \cdots < X^{G-2} < X^{G-1} = a.$$

The subdomains

$$I_k = \{X: X^{k-1} \leqslant X \leqslant X^k, X \subset I, 1 \leqslant k \leqslant G - 1\}$$

are the finite elements $I = \bigcup_{k=1}^{G-1} I_k$, and we denote

$$h_k = \mathrm{dia}\, I_k = X^k - X^{k-1}$$

and

$$h = \max_{1 \leqslant k \leqslant G-1} h_k\,.$$

The real number h serves as a mesh parameter for finite-element approximations.

Let $\mathscr{P}_k(I_j)$ denote the space of polynomials of degree $\leqslant k$ defined on the interval

I_j of I. Then a general class of *discontinuous finite-element approximations* can be defined as elements of the space

$$\mathscr{H}_h^{m,k}(I, P, Q) = \{V(X): V(X) \in L_2(I) \cap C^m(J_j) \cap \mathscr{P}_k(Q_{ij});$$
$$1 \leqslant j \leqslant N; 1 \leqslant i \leqslant G - 1; Q_{ij} = I_i \cap J_j\}.$$

Here m and k are positive integers, J_j are the shockless subdomains defined by the partition Q, I_i are the finite elements corresponding to partition P, and $\mathscr{P}_k(Q_{ij})$ denotes the space of polynomials of degree $\leqslant k$ on each shockless portion of element I_i. The space $\mathscr{H}_h^{m,k}(I, P, Q)$ is appropriate for approximating velocity fields, but we must ensure that the displacement field itself remain continuous. Thus, the discontinuous finite-element approximation of shock waves is a function U in $\mathscr{H}_h^{m,k}(I, P, Q) \cap C^0(I)$, where $C^0(I)$ is the space of functions continuous on I.

When no discontinuities in the velocities or displacement gradients exist, $\mathscr{H}_h^{m,k}(I, P, Q)$ reduces to the usual space of conforming finite-element interpolants. When discontinuities are present, the character of the discontinuity is defined within each element by a number of parameters. So as to simplify the problem of choosing and determining these parameters, we will limit ourselves to local interpolants with the following properties.

(i)   The finite-element basis functions $\{\phi_\alpha\} = \text{span} \, \mathscr{H}_h^{m,k}(I, P, Q) \cap C^0(I)$ will have compact support in I. Indeed, for any $\phi_\alpha(X)$ there will exist two elements I_α, $I_{\alpha+1}$ such that $\phi_\alpha(X) = 0$ for $X \notin I_\alpha \cup I_{\alpha+1}$. Presumably, this requirement will have a beneficial effect, at least as far as the stability of the scheme is concerned.

(ii)   The discontinuous basis functions vanish at the nodes of the element; on the other hand, their values at any point in an element are uniquely determined by the values of the discontinuous interpolant and possibly its derivatives on each side of the shock.

The following elements represent typical examples of discontinuous approximations.

(i)   *Linear elements.*   The simplest representation of a continuous function with a simple discontinuity in its first derivative is the piecewise linear local finite element representation shown in Fig. 1a. There the wave front is located at a position Y in the element.

The piecewise linear local approximation is characterized by four parameters:

$$U(X) = \begin{cases} a + bX, & X \leqslant Y, \\ c + dX, & X > Y, \end{cases} \tag{4.3}$$

$X \in I_\alpha \subset I$. These parameters are determined in terms of the values $U_1 = U(0)$
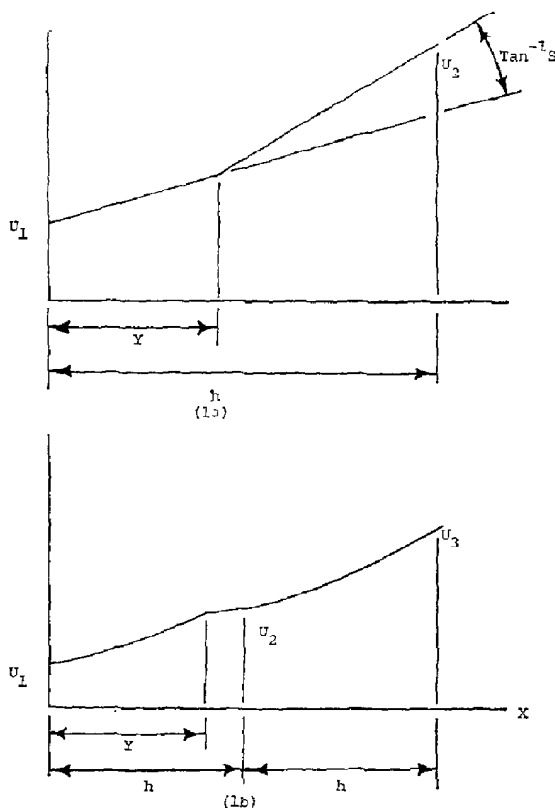
FIG. 1. Examples of piecewise linear and piecewise quadratic approximations.

and $U_2 = U(h)$ at each end of the element and from the fact that U is continuous at Y but dU/dX suffers a *prescribed jump* S:

$$U_1 = a,$$
$$a + bY = c + dY,$$
$$U_2 = c + dh,$$
$$S = [U_X]_Y = b - d.$$

(4.4)

Solving these equations and substituting the results into (4.3) gives

$$U(X) = \sum_{\alpha=1}^{2} U_\alpha \psi_\alpha(X) + S\beta(X) + SY\phi(X),$$

(4.5)

wherein the $\psi_\alpha(X)$ are the *usual* Lagrange finite-element interpolation functions

$$\psi_1(X) = 1 - (X/h), \qquad \psi_2(X) = X/h \tag{4.6}$$

and $\beta(X)$ and $\phi(X)$ are new discontinuous shape functions,

$$\beta(X) = \begin{cases} X, & X \leqslant Y, \\ 0, & X > Y; \end{cases} \qquad \phi(X) = \begin{cases} -X/h, & X \leqslant Y, \\ 1 - (X/h), & X > Y. \end{cases} \tag{4.7}$$

For convenience, we shall refer to this class of functions as the DIS 1 (discontinuous functions of degree 1). They are illustrated in Fig. 2.
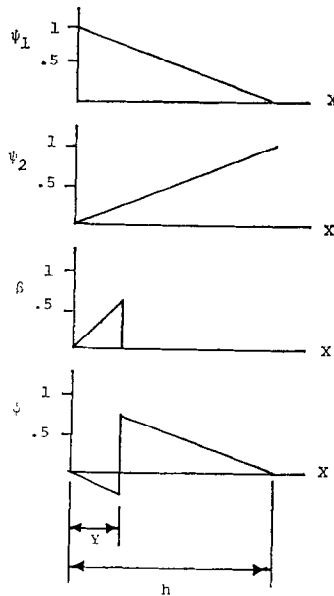
FIG. 2. Discontinuous linear trial functions.

Notice that these functions satisfy the kinematical compatibility conditions (2.12). Let

$$[\![U_X]\!]_Y = S$$

and if we regard S and Y as functions of time t,

$$[\![\partial U/\partial t]\!]_Y = [\![\dot{U}]\!]_Y = \dot{S}[\![\beta]\!]_Y + \dot{S}Y[\![\phi]\!]_Y + S\dot{Y}[\![\phi]\!]_Y = -S\dot{Y}.$$

Thus

$$[\dot{U}]_Y = -\dot{Y}[U_X]_Y, \tag{4.8}$$

as required.

(ii) *Quadratic approximations.* A similar process can be used to construct piecewise quadratic approximations of the type in Fig. 1b. Here we use

$$U = \begin{cases} a + bX + cX^2, & X \leqslant Y; \\ d + eX + fX^2, & X > Y. \end{cases} \tag{4.9}$$

This time, we use two adjacent elements of equal length (for simplicity). Then evaluating (4.9) at $X = 0$, h, and $2h$ and denoting $U(0)$, $U(h)$, and $U(2h)$ by U_1, U_2, U_3, respectively, gives

$$a = U_1,$$
$$d + eh + fh^2 = U_2, \tag{4.10}$$
$$d + 2eh + 4fh^2 = U_3.$$

Since U is continuous at Y,

$$a + bY + cY^2 = d + eY + fY^2. \tag{4.11}$$

Again let S be a parameter identified with the shock strength (4.4) and A be a parameter defined by

$$A = [U_{XX}]_Y. \tag{4.12}$$

Thus, the definition of S and (4.10)–(4.12) are sufficient to uniquely determine the parameters in (4.9). We finally get

$$U(X) = \sum_{\alpha=1}^{3} U_\alpha \psi_\alpha(X) + R\beta(X) + Q\Phi(X) + A\eta(X), \tag{4.13}$$

where $\psi_\alpha(X)$ are the usual continuous quadratic functions and the remaining terms are discontinuous quadratic interpolants:

$$\psi_1(X) = 1 - (3X/2h) + (X^2/2h^2),$$
$$\psi_2(X) = (2X/h) - (X^2/h^2),$$
$$\psi_3(X) = -(X/2h) + (X^2/2h^2),$$
$$\beta(X) = \begin{cases} X, & X \leqslant Y, \\ 0, & X > Y, \end{cases}$$
$$\Phi(X) = \begin{cases} -(3X/2h) + (X^2/2h^2), & X \leqslant Y, \\ 1 - (3X/2h) + (X^2/2h^2), & X > Y, \end{cases} \tag{4.14}$$
$$\eta(X) = \begin{cases} \tfrac{1}{2}X^2, & X \leqslant Y, \\ 0, & X > Y. \end{cases}$$

We shall refer to these functions as the DIS 2 family. They are illustrated in Fig. 3.

The generalized coordinates R and Q in (4.13) are defined as

$$R = S - AY,$$
$$A = SY - \tfrac{1}{2}AY^2. \tag{4.15}$$

It remains to be proved that this choice of interpolants satisfies the proper kinematical compatibility conditions at the shock front. Observe that

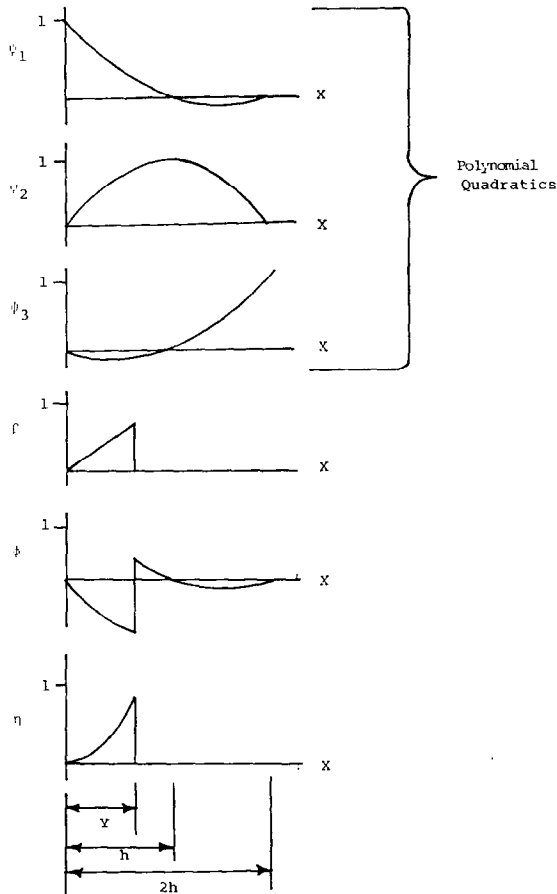$$[\![U_x]\!]_Y = (S - AY)[\![\beta_x]\!]_Y + A[\![\eta_x]\!]_Y = S - AY + AY = S$$

FIG. 3. Discontinuous quadratic trial functions with discontinuity on left side of internal node.

and

$$[\![\dot{U}]\!] = (\dot{S} - \dot{A}X - A\dot{Y})[\![\beta]\!] + (\dot{S}Y + S\dot{Y} - \tfrac{1}{2}\dot{A}Y^2 - AY\dot{Y})[\![\Phi]\!]_Y + \dot{A}[\![\eta]\!]_Y = -S\dot{Y}.$$

Thus

$$[\![\dot{U}]\!]_Y = \dot{Y}[\![U_X]\!]_Y,$$

as required. This means that the *first-order kinematical compatibility* conditions are satisfied.

We use the space $\mathscr{H}_h^{m,k}(I, P, Q) \subset \mathscr{H}$ to define a Galerkin approximation consistent with (3.14). This approximation is the *semidiscrete finite-element/Galerkin method for shock propagation* and is defined as follows. Find $U \in \mathscr{H}_h^{m,k}(I, P, Q) \cap C^0(I)$ such that

$$\sum_{i=1}^{N} \int_{J_i} [(\rho\ddot{U} - f)W + \sigma W_X] \, dX + \sum_{i=1}^{N-1} (\rho V_i [\![\dot{U}]\!]_{Y_i} \, \overline{W}_i - \bar{\sigma}_i [\![W]\!]_{Y_i})$$

$$= \{\sigma(\cdot, t) \, W(\cdot)\}|_{X=0}^{X=a}, \qquad \forall W \in \mathscr{H}_h^{m,k}(I, P, Q). \tag{4.16}$$

5. MODELS OF THE PARTICLE ACCELERATION FIELD

In this section we begin a discussion of the implementation of the semidiscrete finite-element/Galerkin method (4.16) using the discontinuous trial functions introduced in Section 4. We emphasize here the linear trial functions (the DIS 1 set). In particular, we consider here models of the acceleration field.

For convenience in notation we define a new trial function $\chi = \beta + Y\phi$. Then the displacement approximation corresponding to (4.5) is

$$U(X) = \sum_{\alpha=1}^{2} U_\alpha \psi_\alpha(X) + S\chi(X). \tag{5.1}$$

We differentiate (5.1) twice with respect to time and evaluate the resulting expression at time point $t = n \, \Delta t$ to obtain the acceleration at this time point.

$$\ddot{U}^n(X) = \sum_{\alpha=1}^{2} \ddot{U}_\alpha{}^n \psi_\alpha(X) + \ddot{S}^n \chi^n(X) + 2\dot{S}^n \dot{Y}^n \phi^n(X) + S^n \ddot{Y}^n \phi^n(X). \tag{5.2}$$

An approximation can be obtained for $\ddot{U}^n(X)$ by introducing various difference approximations for the first and second temporal derivatives on the right-hand

side of (5.2). We call this the *first inertial approximation*, and it is defined as follows.

$$\ddot{U}^n(X) = \sum_{\alpha=1}^{2} \left(\frac{U_\alpha^{n+1} - 2U_\alpha{}^n + U_\alpha^{n-1}}{\Delta t^2} \right) \psi_\alpha(X) + \left(\frac{S^{n+1} - 2S^n + S^{n-1}}{\Delta t^2} \right) \chi^n(X)$$

$$+ 2 \left(\frac{S^n - S^{n-1}}{\Delta t} \right) \left(\frac{Y^n - Y^{n-1}}{\Delta t} \right) \phi^n(X)$$

$$+ S^n \left(\frac{Y^{n+1} - 2Y^n + Y^{n-1}}{\Delta t^2} \right) \phi^n(X). \tag{5.3}$$

A simpler expression can be obtained in cases when the third and fourth terms on the right-hand side in (5.2) can be neglected (by physical arguments) compared to the first two terms on the right-hand side. We call this the *second inertial approximation*. It is defined as follows.

$$\ddot{U}^n(X) = \sum_{\alpha=1}^{2} \left(\frac{U_\alpha^{n+1} - 2U_\alpha{}^n + U_\alpha^{n-1}}{\Delta t^2} \right) \psi_\alpha(X) + \left(\frac{S^{n+1} - 2S^n + S^{n-1}}{\Delta t^2} \right) \chi^n(X). \tag{5.4}$$

A third alternative acceleration term can be obtained by approximating $\ddot{U}(X)$ directly using central differences. This we call the *third intertial approximation*. It is defined by the expression

$$\ddot{U}^n(X) = \frac{U^{n+1} - 2U^n + U^{n-1}}{\Delta t^2} = \sum_{\alpha=1}^{2} \left(\frac{U_\alpha^{n+1} - 2U_\alpha{}^n + U_\alpha^{n-1}}{\Delta t^2} \right) \psi_\alpha(X)$$

$$+ \frac{S^{n+1}\chi^{n+1}(X) - 2S^n\chi^n(X) + S^{n-1}\chi^{n-1}(X)}{\Delta t^2}. \tag{5.5}$$

Several approximation schemes can be developed from these alternative inertial formulations. We will discuss these alternate approximation schemes in the following sections.

6. THE EXPLICIT WAVE POSITION METHOD

Initially we consider a model which uses the first inertial approximation. We essentially use the formulation presented in Section 4 (in particular, Eq. (4.16)), except that we apply the equations on the element level. We consider a one-dimensional finite element I_e which is pertitioned into two disjoint shockless

domains J_{e_1} and J_{e_2} as shown in Fig. 4. We introduce (5.2) into (4.16) and select W from the set $\{\psi_1, \psi_2, \beta, \phi\}$. The following system of equations is obtained.

$$
\sum_{\alpha=1}^{2} M_{\alpha\beta} \left(\frac{U_\alpha^{n+1} - 2U_\alpha^{\;n} + U_\alpha^{n-1}}{\Delta t^2} \right) + B_\beta^{\;n} \left(\frac{S^{n+1} - 2S^n + S^{n-1}}{\Delta t^2} \right)
$$

$$
+ C_\beta^{\;n} S^n \left(\frac{Y^{n+1} - 2Y^n + Y^{n-1}}{\Delta t^2} \right) + \sum_{\imath=1}^{2} \int_{J_{e_i}^n} \sigma^n \psi_{\beta,X} \, dX
$$

$$
= -2C_\beta^{\;n} \left(\frac{S^n - S^{n-1}}{\Delta t} \right) \left(\frac{Y^n - Y^{n-1}}{\Delta t} \right) + \rho V^2 S^n \bar{\psi}_\beta(Y^n) + f_\beta + S_\beta^{\;n}, \qquad (6.1)
$$

$$
\sum_{\alpha=1}^{2} D_\alpha^{\;n} \left(\frac{U_\alpha^{n+1} - 2U_\alpha^{\;n} + U_\alpha^{n-1}}{\Delta t^2} \right) + E^n \left(\frac{S^{n+1} - 2S^n + S^{n-1}}{\Delta t^2} \right)
$$

$$
+ F^n S^n \left(\frac{Y^{n+1} - 2Y^n + Y^{n-1}}{\Delta t^2} \right) + \sum_{\imath=1}^{2} \int_{J_{e_i}^n} \sigma^n \beta^n_{,X} \, dX
$$

$$
= -2F^n \left(\frac{S^n - S^{n-1}}{\Delta t} \right) \left(\frac{Y^n - Y^{n-1}}{\Delta t} \right) + \rho V_n^2 S^n \bar{\beta}^n + \bar{\sigma}^n [\![\beta^n]\!]_{Y^n} + R^n, \qquad (6.2)
$$

$$
\sum_{\alpha=1}^{2} H_\alpha^{\;n} \left(\frac{U_\alpha^{n+1} - 2U_\alpha^{\;n} + U_\alpha^{n-1}}{\Delta t^2} \right) + Q^n \left(\frac{S^{n+1} - 2S^n + S^{n-1}}{\Delta t^2} \right)
$$

$$
+ T^n S^n \left(\frac{Y^{n+1} - 2Y^n + Y^{n-1}}{\Delta t^2} \right) + \sum_{\imath=1}^{2} \int_{J_{e_i}^n} \sigma^n \phi^n_{,X} \, dX
$$

$$
= -2T^n \left(\frac{S^n - S^{n-1}}{\Delta t} \right) \left(\frac{Y^n - Y^{n-1}}{\Delta t} \right) + \rho V_n^2 S^n \bar{\phi}^n + \bar{\sigma}^n [\![\phi^n]\!]_{Y^n} + Z^n, \qquad (6.3)
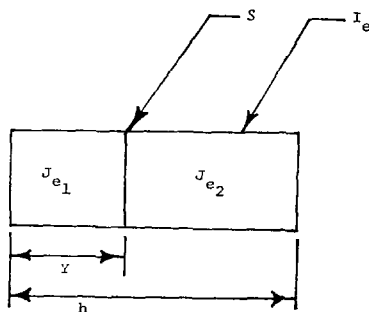$$

FIG. 4.   One-dimensional finite element with a singular surface $\mathscr{S}$.

where

$$M_{\alpha\beta} = \int_{I_e} \psi_\alpha(X)\,\psi_\beta(X)\,dX, \qquad C_\beta{}^n = \sum_{i=1}^{2} \int_{J_{e_i}^n} \phi^n(X)\,\psi_\beta(X)\,dX;$$

$$B_\beta{}^n = \sum_{i=1}^{2} \int_{J_{e_i}^n} \chi^n(X)\,\psi_\beta(X)\,dX, \qquad D_\alpha{}^n = \sum_{i=1}^{2} \int_{J_{e_i}^n} \psi_\alpha(X)\,\beta^n(X)\,dX;$$

$$E^n = \sum_{i=1}^{2} \int_{J_{e_i}^n} \chi^n(X)\,\beta^n(X)\,dX, \qquad f_\beta = \int_{I_e} f\psi_\beta\,dX;$$

$$F^n = \sum_{i=1}^{2} \int_{J_{e_i}^n} \phi^n(X)\,\beta^n(X)\,dX, \qquad S_\beta{}^n = \sigma^n\psi_\beta \big|_0^{h_e};$$

$$H_\alpha{}^n = \sum_{i=1}^{2} \int_{J_{e_i}^n} \psi_\alpha(X)\,\phi^n(X)\,dX, \qquad R^n = \sum_{i=1}^{2} \int_{J_{e_i}^n} f\beta^n\,dX;$$

$$Q^n = \sum_{i=1}^{2} \int_{J_{e_i}^n} \chi^n(X)\,\phi^n(X)\,dX, \qquad Z^n = \sum_{i=1}^{2} \int_{J_{e_i}^n} f\phi^n\,dX;$$

$$T^n = \sum_{i=1}^{2} \int_{J_{e_i}^n} \phi^n(X)\,\phi^n(X)\,dX.$$

We normally set

$$V_n = (Y^n - Y^{n-1})/\Delta t. \tag{6.4}$$

This scheme is started with a forward difference approximation at time point $t = 0$.

The scheme (6.1–6.4) will be characterized as an *explicit shock position method*. The position of the shock is a dependent variable. Essentially we integrate the second time derivative of the shock position Y twice to obtain the change in position of the shock. Presumably this formulation should allow for more accurate determination of the shock position and should more consistently bring the shock position into the formulation since it appears as a dependent variable. Unfortunately, this scheme appears to be unstable in sample calculations, and we suspect that a more judicious choice of the trial functions and the approximation for the temporal operator is necessary to produce a stable scheme. Nevertheless, the general method behind this approximation seems to be the most natural, and we hope that future computations can improve its performance.

7. The Implicit Shock Position Method

We can obtain another shock fitting method by using the second approximation (Eq. (5.4)). Introducing (5.4) into (4.16) and selecting W from $\{\psi_1, \psi_2, \beta\}$, we get

$$\sum_{\alpha=1}^{2} M_{\alpha\beta} \left(\frac{U_\alpha^{n+1} - 2U_\alpha{}^n + U_\alpha^{n-1}}{\Delta t^2} \right) + B_\beta{}^n \left(\frac{S^{n+1} - 2S^n + S^{n-1}}{\Delta t^2} \right) + \sum_{i=1}^{2} \int_{J_{e_i}^n} \sigma^n \psi_{\beta,X} \, dX$$

$$= \rho V_n^2 S^n \bar{\psi}_\beta(Y^n) + f_\beta + S_\beta{}^n, \tag{7.1}$$

$$\sum_{\alpha=1}^{2} D_\alpha{}^n \left(\frac{U_\alpha^{n+1} - 2U_\alpha{}^n + U_\alpha^{n-1}}{\Delta t^2} \right) + E^n \left(\frac{S^{n+1} - 2S^n + S^{n-1}}{\Delta t^2} \right) + \sum_{i=1}^{2} \int_{J_{e_i}^n} \sigma^n \beta^n{}_X \, dX$$

$$= \rho V_n^2 S^n \bar{\beta}^n + \bar{\sigma}^n [\![\beta^n]\!]_{Y^n} + R^n. \tag{7.2}$$

An additional equation is required to define Y^n. We set

$$(Y^{n+1} - Y^n)/\Delta t = V_n, \tag{7.3}$$

where

$$V_n = ([\![\sigma^n]\!]_{Y^n}/\rho S^n)^{1/2}. \tag{7.4}$$

This expression for the shock speed is obtained by evaluating (2.13) at time point $t = n \, \Delta t$. We call (7.1)–(7.4) an *implicit shock position scheme.*

In the implicit shock position method the velocity of the shock is defined by a relationship (7.4) valid only at the wave front and only involves the data at time point $t = n \, \Delta t$. In the explicit shock position method the velocity of the shock is defined by integrating the acceleration of the shock. The acceleration of the shock is defined in turn by global balance laws and is determined from the solution at time point $t = n \, \Delta t$ and time point $t = (n - 1) \, \Delta t$. Thus there is a significant difference between the two approximations. As mentioned in Section 6 the explicit shock position method seems to be unstable for the specific choice of trial functions and integration algorithm used there. However, the implicit shock fitting method is stable for reasonable choices of the discretization parameters. Thus it has been our main tool in numerical calculations.

An assumption in the implicit shock fitting method is that the last two terms on the right-hand side in (5.2) are small compared to the first two. In cases in which this assumption cannot be justified we can still construct an implicit shock fitting method using the third inertial approximation. Introducing (5.5) into (4.16) and selecting W from $\{\psi_1, \psi_2, \beta\}$, we get

$$\sum_{\alpha=1}^{2} M_{\alpha\beta} \left(\frac{U_\alpha^{n+1} - 2U_\alpha{}^n + U_\alpha^{n-1}}{\Delta t^2} \right) + \frac{1}{\Delta t^2} B_\beta^{n+1} S^{n+1} - \frac{2}{\Delta t^2} B_\beta{}^n S^n$$

$$+ \frac{1}{\Delta t^2} B_\beta^{n-1} S^{n-1} + \sum_{i=1}^{2} \int_{J_{e_i}^n} \sigma^n \psi_{\beta,X} \, dX = \rho V_n^2 S^n \bar{\psi}_\beta(Y^n) + f_\beta + S_\beta{}^n, \tag{7.5}$$

$$\sum_{\alpha=1}^{2} D_\alpha{}^n \left(\frac{U_\alpha^{n+1} - 2U_\alpha{}^n + U_\alpha^{n-1}}{\Delta t^2} \right) + \frac{1}{\Delta t^2} K^n S^{n+1} - \frac{2}{\Delta t^2} E^n S^n$$

$$+ \frac{1}{\Delta t^2} L^n S^{n-1} + \sum_{i=1}^{2} \int_{J_{e_i}^n} \sigma^n \beta^n{}_X \, dX = \rho V_n{}^2 S^n \bar\beta^n + \bar\sigma^n [\![\beta^n]\!]_{Y^n} + R^n, \quad (7.6)$$

$$(Y^{n+1} - Y^n)/\Delta t = V_n, \qquad (7.7)$$

$$V_n = ([\![\sigma^n]\!]_{Y^n}/\rho S^n)^{1/2}, \qquad (7.8)$$

where

$$K^n = \sum_{i=1}^{2} \int_{J_{e_i}^n} \chi^{n+1}(X) \, \beta^n(X) \, dX, \qquad (7.9)$$

$$L^n = \sum_{i=1}^{2} \int_{J_{e_i}^n} \chi^{n-1}(X) \, \beta^n(X) \, dX. \qquad (7.10)$$

Implementation of this method is only slightly more complicated than the implementation of the implicit shock position method and both use the same initial conditions and starting procedure.

8. The Global Formulation for Wave and Shock Propagation

In Section 7 equations of motion valid for finite elements containing shock waves were developed. In the global model for shock propagation we use this element as a special element which effectively forms a boundary layer around the shock and connects shockless regions of ordinary finite elements. In Fig. 5 we show a typical example of a one-dimensional bar containing a single shock wave. The bar is divided into 16 finite elements whose nodes correspond to fixed material coordinates; i.e., we use a Lagrangian coordinate system for the elements. The shock wave forms a moving surface in an element designated as the special element. All other elements in the model are standard. When the shock surface crosses interelement boundaries the special element also moves and the previous special element reverts to a standard finite element. When the wave passes an external node of an element during a specific time step, there is, of course, a discontinuity in the velocity of the node at some point during the time step. It is essential to represent this phenomenon accurately, and we use a special integration procedure
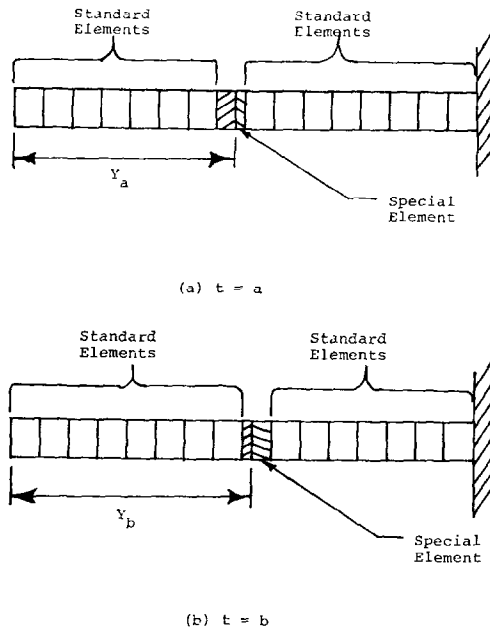
(a) t = a

(b) t = b

FIG. 5.   Finite element model with special element as a boundary layer at the singular surface.

when this happens. Suppose the node lies at a point Z relative to the origin of the global coordinate system. Then let

$$\gamma = (Y^{n+1} - Z)/(Y^{n+1} - Y^n), \tag{8.1}$$

$$\Delta t' = \gamma \, \Delta t, \tag{8.2}$$

$$\Delta t'' = (1 - \gamma) \, \Delta t. \tag{8.3}$$

Then the displacement as the wave reaches the external node is

$$\overline{U}^n = U^n \frac{(\Delta t'' + \Delta t)}{\Delta t} - U^{n-1} \frac{\Delta t''}{\Delta t} + \frac{\Delta t''(\Delta t + \Delta t'') \, U^n}{2} \tag{8.4}$$

and an approximation for the displacement of the external node at the end of the time step is

$$U^{n+1} = \overline{U}^n - V_n S^{n+1} \, \Delta t'. \tag{8.5}$$

In the next time step we must again use a special procedure to compute the displacement of this node. We use

$$U^{n+2} = U^{n+1} \frac{(\Delta t + \Delta t')}{\Delta t'} - \frac{\overline{U}^n \Delta t}{\Delta t'} + \frac{\Delta t(\Delta t + \Delta t') \, \ddot{U}^{n+1}}{2} .$$

In the global formulation we must introduce a special procedure to handle the reflection of nonlinear waves. It is necessary to determine the displacement gradient and the intrinsic velocity of the wave after reflection. In the shock fitting method we require that the momentum jump condition (2.11)$_4$ and the kinematical compatibility condition (2.12) be satisfied. Noting that after reflection the particle velocity at the wall must be zero, these conditions imply that

$$-\rho \frac{du^-}{dX} V^2 + \rho \frac{du^+}{dX} V^2 - \sigma^+ + \sigma^- = 0,$$

$$V \frac{du^-}{dX} - V \frac{du^+}{dX} + \dot{u}^- = 0. \tag{8.7}$$

dU^-/dX, σ^-, and $\dot{u}^-$ are known properties of the incoming wave, and du^+/dX and V are the unknowns of the problem.

Equation (8.7) can be solved by the Newton–Raphson method. Let $\mathbf{x} = \{V, du^+/dX\}$. Then let

$$\mathbf{F} = \begin{cases} -\rho \dfrac{du^-}{dX} x_1{}^2 + \rho x_2 x_1{}^2 - \sigma^+ + \sigma^-, \\[2mm] x_1 \dfrac{du^-}{dX} - x_1 x_2 + \dot{u}^-. \end{cases} \tag{8.8}$$

Then as an iterative procedure we require that

$$\mathbf{x}^{n+1} = \mathbf{x}^n - (\mathbf{J}^n)^{-1} \mathbf{F}^n, \tag{8.9}$$

where $\mathbf{J}$ is the Jacobian matrix defined by

$$\mathbf{J} = [\partial F_i/\partial x_j]. \tag{8.10}$$

If we consider a Mooney material [4] in which the first Piola–Kirchhoff stress σ is defined by

$$\sigma = 2(C_1\lambda + C_2)[1 - (1/\lambda^3)], \tag{8.11}$$

where $\lambda = 1 + u_X$, the following explicit expressions for the entries in $\mathbf{J}$ can be developed:

$$J_{11} = -2\rho(du^-/dX) x_1 + 2\rho x_2 x_1\,,$$

$$J_{12} = x_1{}^2 - 2C_1 - \frac{4C_1}{(1 + x_2)^3} - \frac{6C_2}{(1 + x_2)^4}\,, \tag{8.12}$$

$$J_{21} = (du^-/dX) - x_2\,,$$

$$J_{22} = -x_1\,.$$

We have obtained very good results by using the reflected wave for a linear material as an initial guess to start the iteration. Then we set

$$x_1{}^0 = -\bar{V},$$
$$x_2{}^0 = (du^-/dX) + S,$$
(8.13)

where $\bar{V}$ is the intrinsic velocity of the wave prior to reflection and S is the shock strength. Convergence occurs in around seven steps of the procedure (8.9). As a final step in defining the reflected wave, we set

$$S = (du^-/dX) - x_2$$
(8.14)

and proceed with the calculations.

9. A LINEAR TEST PROBLEM

In order to demonstrate the ideas of this paper in calculation of a problem for which an exact solution is known, we consider here the case of linear wave propagation in which a jump in stress is prescribed at the wave front by applying a step load to a one-dimensional linear elastic bar. The physical parameters of the problem are shown in Fig. 6. In Fig. 7, we compare the stress calculated by the shock fitting method with linear trial functions with the profiles based on a central difference approximation and a parabolic regularization method (see [5]). In Fig. 8, the stress wave computed by our discontinuous Galerkin method is shown at several time
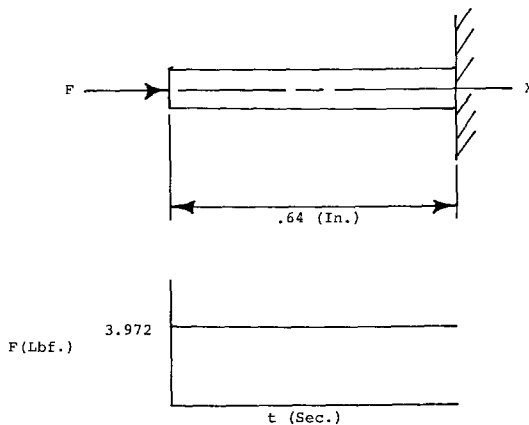
FIG. 6. Physical model for propagation of a linear wave. Physical parameters: density = 1.0×10^{-4} lbf-sec^2/in^4, area = 0.0314 in^2, modulus of elasticity = 63.25 lbf/in^2, length = 0.64 in.
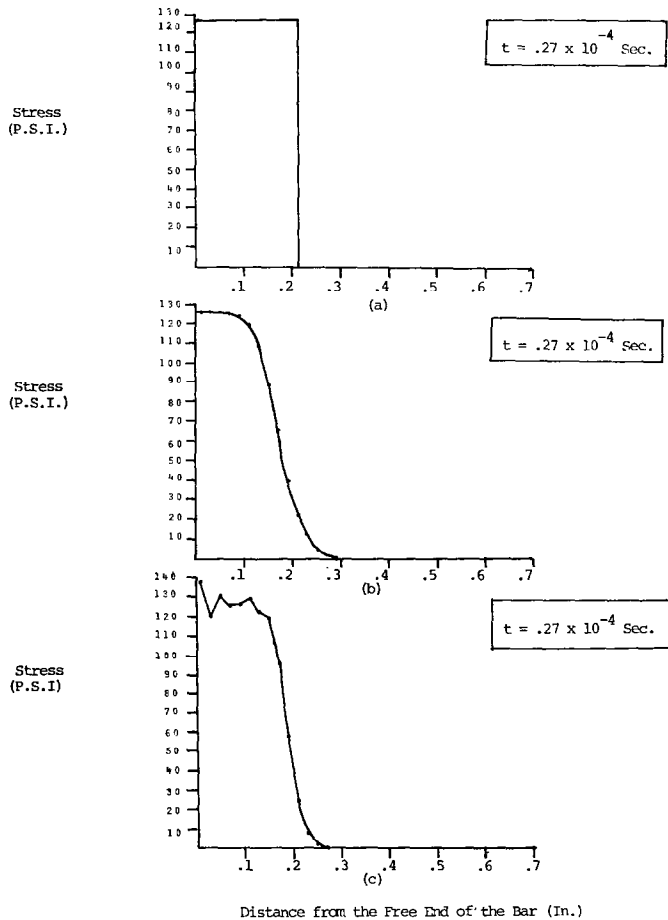
FIG. 7. Linear wave propagation calculation by several methods.

points during the propagation of the wave both before and after reflection. The shock fitting solution is exact for this problem and the marked improvement provided by the use of the method is clear.

We note that for this problem the phenomenon of "infinite wave speed" of Galerkin models did not occur. That is, the stress in front of the wave was absolutely zero. This can be attributed to the following factors. First, the formulation includes the wave implicitly. Second, there is no acceleration in this problem; that is, the velocity is piecewise constant. Within the element we can model this piecewise form exactly. Thus, the region in front of the wave is not strained.
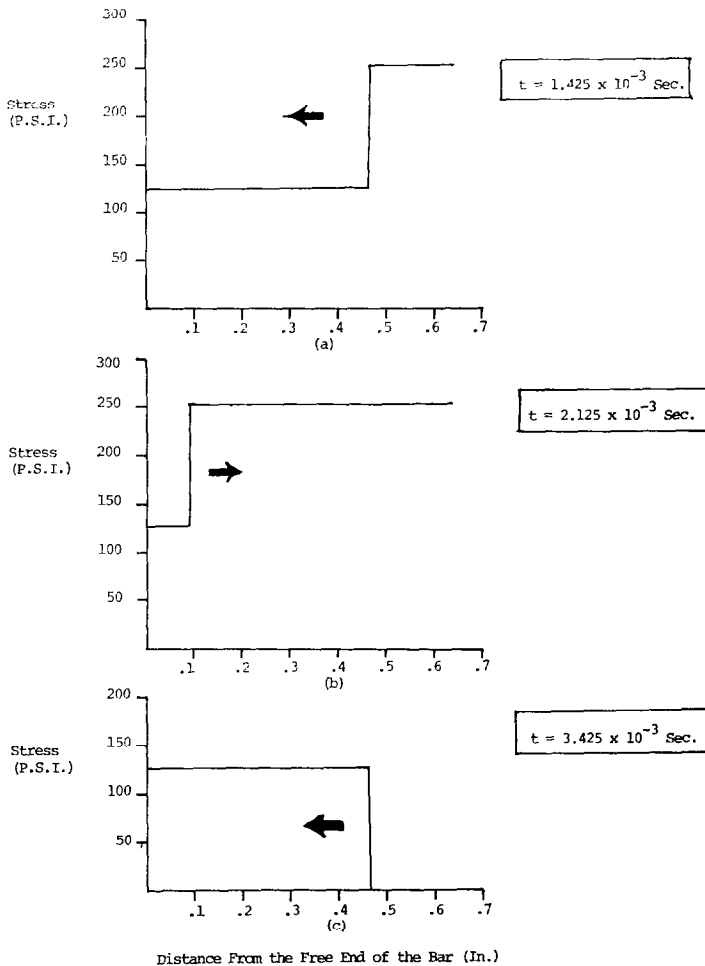
FIG. 8.   Linear wave propagation by the shock fitting method.

10. THE GROWTH OF SHOCK WAVES

In order to demonstrate the use of the shock fitting scheme, we consider the growth of a compression shock wave in a one-dimensional elastic bar of Mooney material. The constitutive equation for the Mooney material is given in (8.11). The physical parameters of the problem as well as the forcing function are shown in Fig. 9.
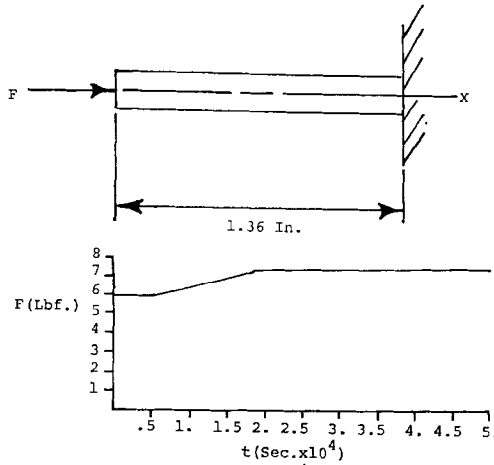
FIG. 9. Physical and model parameters for calculation of compression shock wave in a one-dimensional bar of Mooney material. Physical parameters: density $= 1.0 \times 10^{-4}$ lbf-sec^2/in^4, area $= .0314$ in^2, $C_1 = 24.0$ lbf/in^2, $C_2 = 1.5$ lbf/in^2, length $= 1.36$ in, initial force $= 5.9346$ lbf, final force $= 7.2220$ lbf. Model parameters (shock fitting scheme): $h = 0.02$ in $DT = 1.5 \times 10^{-7}$ sec.

In the calculations to be presented here the *implicit shock* position method was used with the linear trial functions (the DIS 1 set). The same equations as described in Section 10 were used in the calculations with one exception. In the standard elements an explicit artificial viscosity term of the following form was added to the equations for each element.

$$\Delta t^{0.8} \int_{I_e} \frac{\partial \sigma(u_X)}{\partial u_X}\bigg|_{u=U^n} \frac{u_X^n - u_X^{n-1}}{\Delta t} \psi_{\beta,X}\, dX, \qquad \beta = 1, 2. \tag{10.1}$$

This term was added to avoid the consideration of the acceleration waves induced in the bar when the applied load shown in Fig. 9 has a discontinuity in slope. Since our primary goal here is to model the shock wave, we smeared the acceleration wave rather than treated it through some fitting technique for acceleration waves. No artificial viscosity was used in the special element at the shock wave.

In Fig. 10 the variation of the shock strength S is given as a function of time. It is compared to the theoretical upper bound of the shock strength which would be attained if there was no dissipation of the strength of shock in the shock propagation process. In Fig. 11 the variation of the intrinsic speed of the shock wave is plotted as a function of time. We note here one of the advantages of the finite-element/shock fitting scheme. The shock strength and intrinsic wave speed are extremely accessible in that they are dependent variables in the finite-element model.
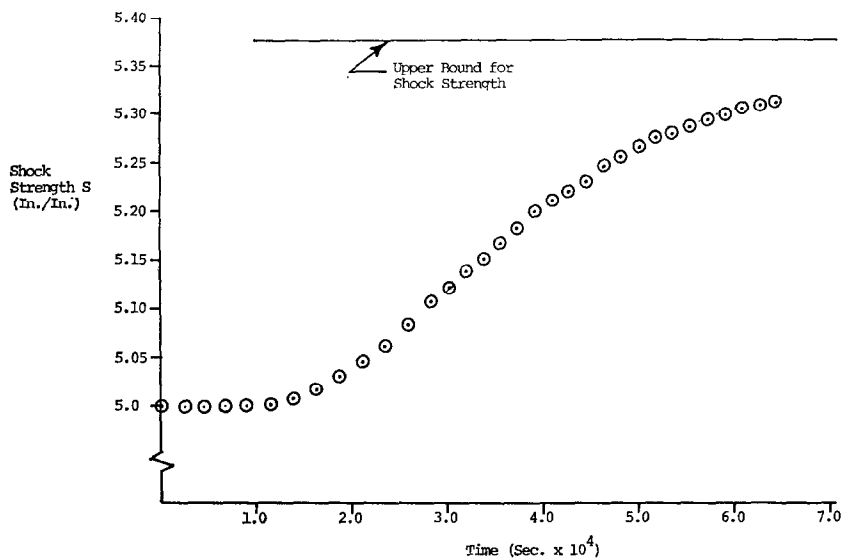
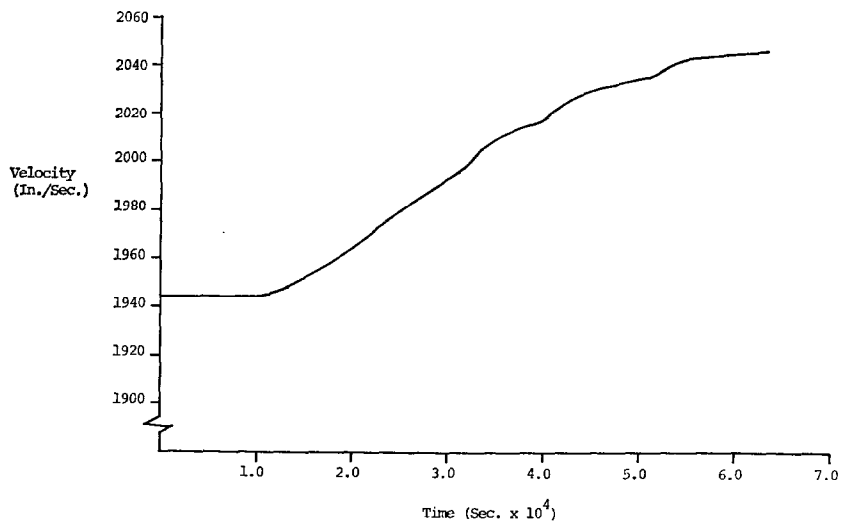FIG. 10.   Growth of shock strength for the compression shock computed by the shock fitting scheme.

FIG. 11.   Intrinsic velocity of the compression shock wave computed by the shock fitting scheme.
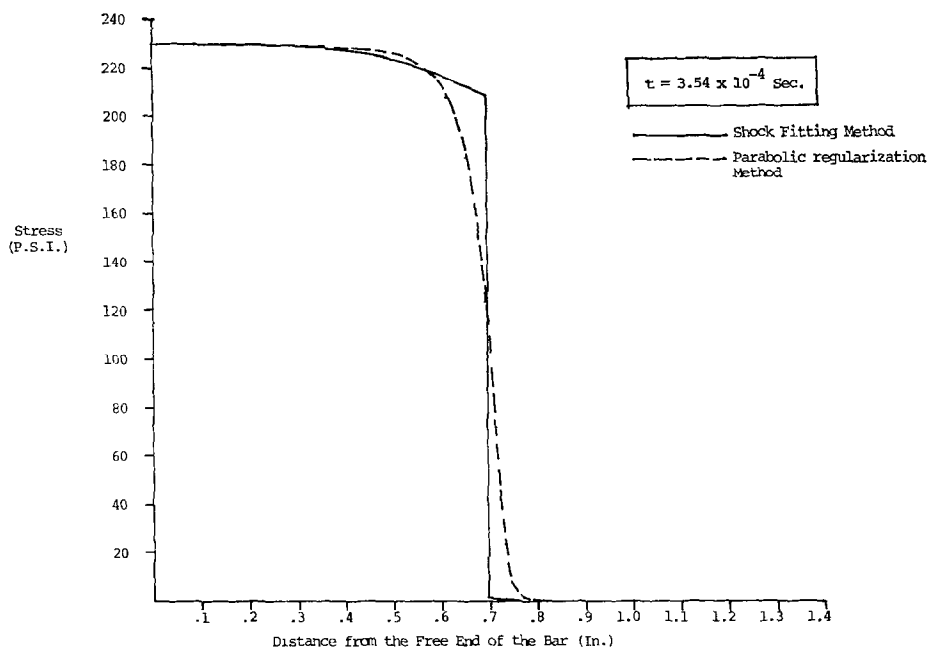
FIG. 12.   A comparison of the shock fitting solution and the parabolic regularization solution at $t = 3.54 \times 10^{-4}$ sec.
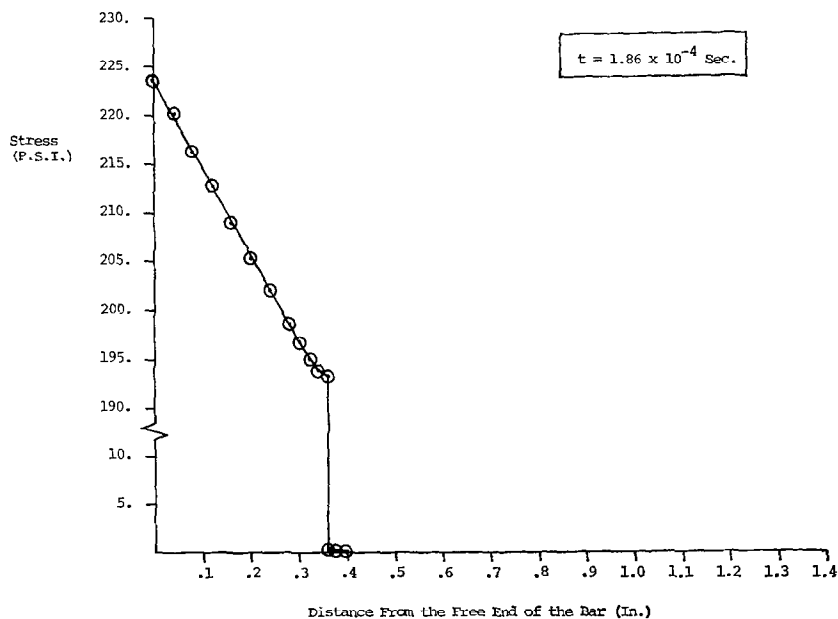

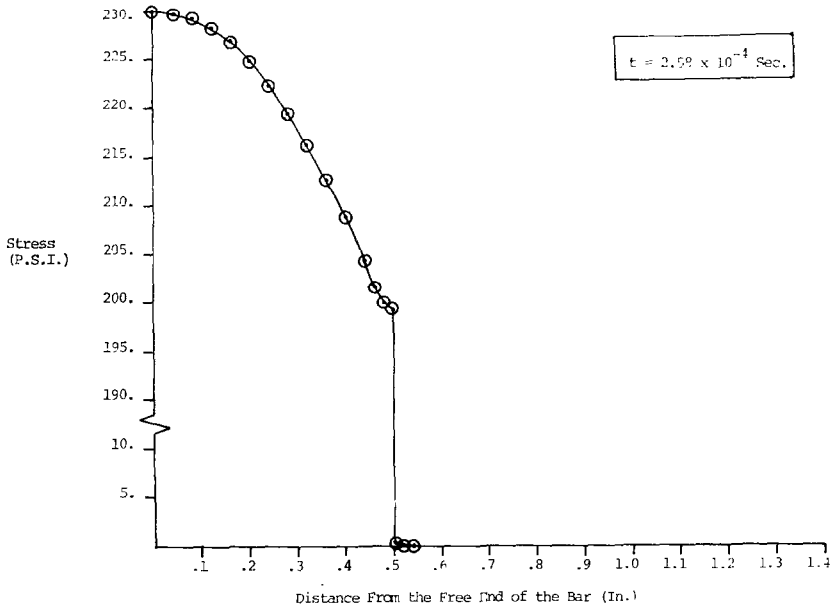FIG. 13a.   Growth of a compression shock wave computed by the shock fitting scheme.

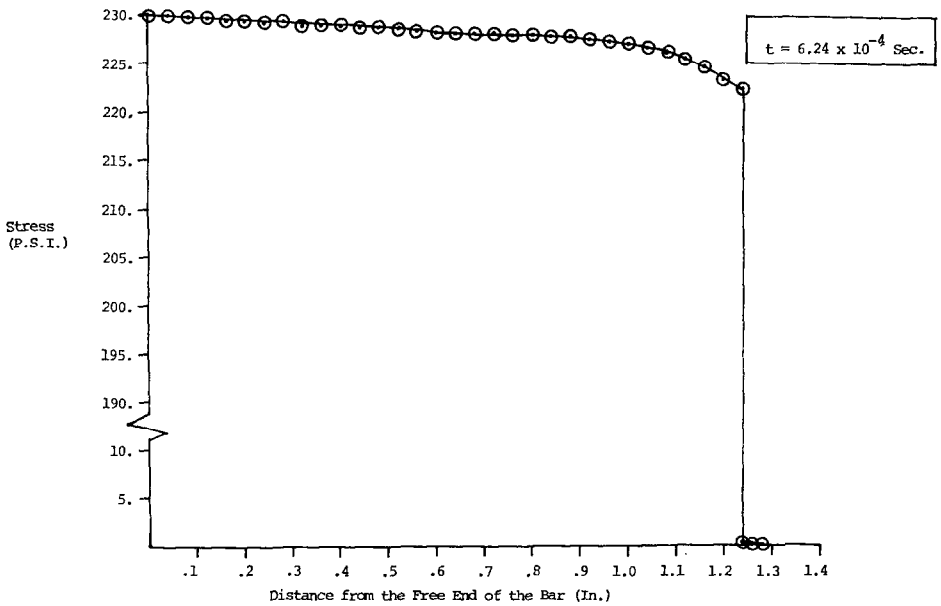FIG. 13b.   Growth of a compression shock wave computed by the shock fitting scheme.

FIG. 13c.   Growth of a compression shock wave computed by the shock fitting scheme.

To provide some basis for evaluating the qualitative and quantitative behavior of the finite-element/shock fitting scheme in application to the above problem, the same calculation was performed with a shock smearing scheme (in this case, the parabolic regularization scheme of [5] with $\alpha = 0.8$.). In Fig. 12 we compare the parabolic regularization and the shock fitting method at time point $t = 3.54 \times 10^{-4}$ sec. In Fig. 13 the shock fitting solution is pictured at various time points. The detailed structure of the shock wave is captured by the shock fitting scheme. However, the parabolic regularization method distorts the shock wave and provides no indication of the true strength of the shock.

Concerning the inertial approximation and in particular the mass matrices used in these calculations, we make the following comments. In the standard elements we used a "lumped mass matrix." In the special elements we used the mass matrix developed from inertial approximation (5.4). The mass matrix for the special element is thus "distributed." We do not yet know how to form a "lumped mass" matrix for the special element. The construction of such a mass matrix would be highly desirable since the use of the consistent mass matrix causes a slight inertial coupling across the wave front. The nonzero stress in front of the wave in Fig. 13 is caused by this inertial coupling.

Next we consider the reflection of a nonlinear wave from a rigid wall in a one-dimensional rod of Mooney material. The physical parameters are presented in Fig. 14. In Fig. 15 the shock fitting solution is presented before and after reflection. In Fig. 16 the same problem is presented except the calculations are performed with a shock smearing method (again the parabolic regularization method [5] with
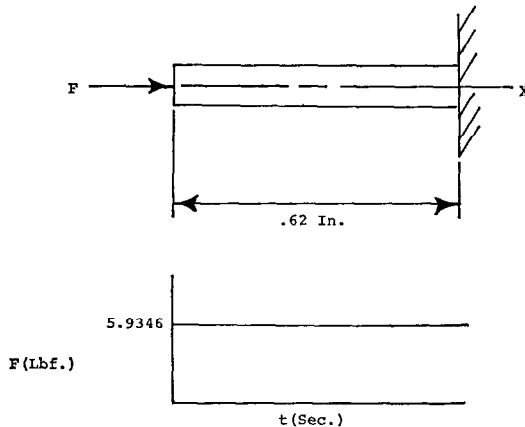

FIG. 14. Physical parameters for the calculation of reflection of a nonlinear wave. Physical parameters: density $= 1.0 \times 10^{-4}$ lbf-sec^2/in^4, area $= .0314$ in^2, $C_1 = 24.0$ lbf/in^2, $C_2 = 1.5$ lbf/in^2, length $= 0.62$ in.
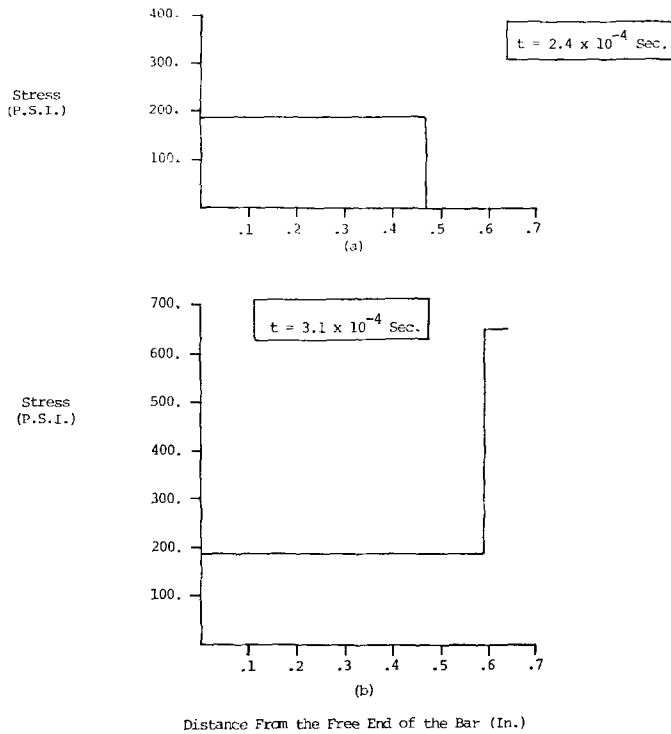
FIG. 15. Reflection of a nonlinear wave by the shock fitting method.

$\alpha = 0.8$). Figures 16a and b correspond to the time points presented in Fig. 15 for the shock fitting reflected wave is fully developed (650.4 psi); however, the parabolic regularization reflected wave is just beginning to develop. In Fig. 16c at $t = 3.6 \times 10^{-4}$ sec the parabolic regularization reflected wave is fully developed (625.0 psi). The effect of the shock smearing/parabolic regularization scheme on the reflection is to introduce a phase error in the calculations. This error causes the reflected wave to reach its peak well after the actual wave. One the other hand, the shock fitting model gives a detailed description of the reflection process.

CONCLUSION

In this paper the solution of problems of shock propagation in nonlinear elastic solids using finite element models with discontinuous trial functions has been demonstrated. The ideas and techniques developed here are, however, much
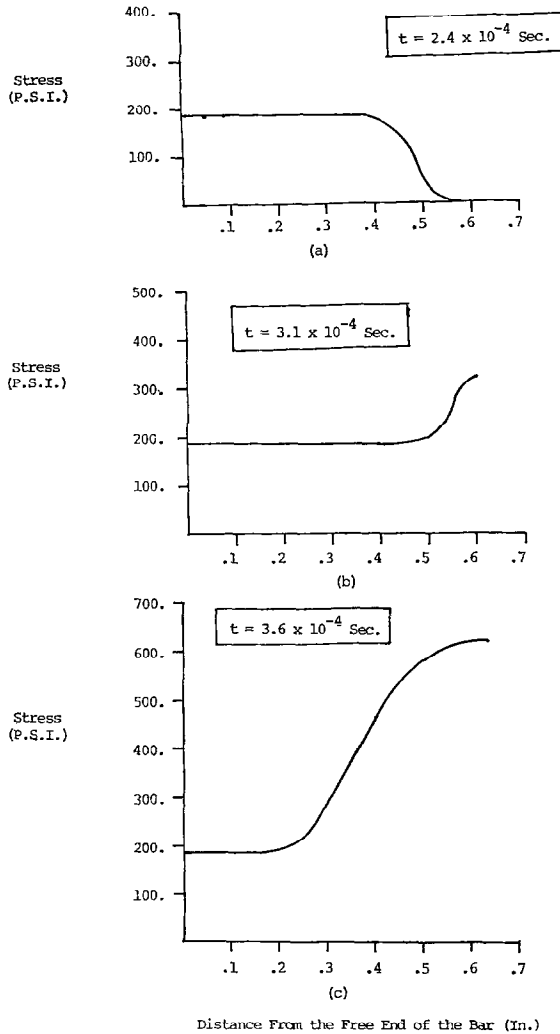
FIG. 16. Reflection of a nonlinear wave by the parabolic regularization method ($\alpha = 0.8$).

more general. These methods could be applied, for example, to the propagation of shocks in fluid media and to the propagation of higher-order waves (with discontinuities in higher derivatives of the solution) in solids or fluids.

REFERENCES

1. L. C. WELLFORD, JR., AND J. T. ODEN, *Comput. Meth Appl. Mech. Eng.* **7**, Nos. 1, 2 (1976), to appear.
2. C. TRUESDELL AND R. TOUPIN, The classical field theories, *in* "Encyclopedia of Physics," Vol. III/1 (S. Flugge, Ed.), pp. 226–793, Springer–Verlag, Amsterdam, 1960.
3. B. COLEMAN, M. GURTIN, AND I. HERRERA, *Arch. Rational Mech. Anal.* **19** (1965), 1–19.
4. M. MOONEY, *J. Appl. Phys.* **11** (1940), 582–592.
5. L. C. WELLFORD AND J. T. ODEN, On Some Ginite Element Methods for Certain Nonlinear Second Order Hyperbolic Equations, TICOM Report 74-7, Texas Institute for Computational Mechanics, Univ. of Texas, Austin, 1974.